

# **STUDIES ON THE REFRACTIVE INDEX OF POLYOLEFINE FILAMENTS WITH SPECIAL REFERENCE TO POLYPROPYLENE FILAMENTS**

by

Hiroshi ISHIKAWA

*Laboratory of Fiber Physics, The Faculty of Textile Science  
and Technology, Shinshu University*

## **I. INTRODUCTION**

In the textile technology, it must be one of important problems that we clarify changes of fiber structures caused by spinning, stretching and heating.

To analysis of these changes, the author applied the Becke's line method, which is known as a famous method for measurement of refractive index of mineral crystal. According to Becke's line method as we known, each of  $n_{//}$  and  $n_{\perp}$  is measured independently. The author, however, has recognized the fact that the interrelation diagram between  $n_{//}$  and  $n_{\perp}$  can be used to measure quantitatively various changes of fine structures of the fibers.

This method is now young, but the author expects that further studies bring the improvements of the textile properties.

## **II. EXPERIMENTAL SAMPLES AND METHODS**

### **A. Preparation of Samples**

Samples were prepared by the following treatments.

- Sample No. 1 ; Commercial sample composed of 300 denier multi-filaments (36 filaments), 250 times spinning draft.  $[\eta]_f=1.0$  (in tetralin at 135°C), molecular weight 34,000~35,000, birefringence (passed 3 years from spinning) 0.006~0.008.
- Sample No. 2 ; This sample was made from No.1 sample treated by cold drawing under the handling stretch machine, stretching speed 6 cm/min. Determination of extension ratios of this sample was done when the sample passed 1.0 hr at relaxed condition after keeping 3 hr at fixed length.
- Sample No. 3 ; The sample was made by heat stretching in Polyethylene-glycohol bath at various temperatures such as 60, 80, 100, 120 and 140°C. Stretching speed about 6 cm/min.
- Sample No. 4 ; This sample was made from No. 1 sample annealed atonically in heated Polyethylene-Glycohol bath at various temperatures such as 60, 80, 100, 120, 140 and 160°C for 30 min.

- Sample No. 5 ; The sample was made from No.2 sample annealed atonically and isometrically in a heated oven at various temperatures for 30 min.
- Sample No. 6 ; The sample was made by such procedure as ; the polymer melted at 270°C and kept this condition for 1.0hr, next extruded at this temperature through a spinneret of circular orifice, (A) the extruded monofilament quenched at 20°C and taken up with a speed of 2 m/min.
- Sample No. 7 ; This is the sample, in which No.6 sample was atonically annealed in a heated oven at various temperatures for 30 min.
- Sample No. 8 ; The sample was made by the same method as the sample No. 6, but differing from it in (A) treatment, in which the extruded monofilaments were quenched in glycerine bath at various temperatures and taken up at a speed of 250 m/min.
- Sample No. 9 ; The sample was made by No. 8 sample which was stretched in a heated oven at 120°C and 140°C.
- Sample No. 10 ; The sample was made by the following method : the polymer melted at 250°C and kept this condition for 1.0 hr, next extruded at 250°C through a spinneret of circular orifice, the extruded monofilaments quenched at 20°C and taken up with

Table 1. Classification of Samples

Treatment Sample	Spinning	Stretching	Heating	
Polypropylene	No. 1 undrawn filament	stretched filament <ul style="list-style-type: none"> <li>No. 2 cold drawing → No. 5</li> <li>No. 3 heat stretching</li> </ul>	{ atonically annealed f. isometrically annealed f.	
				non-stretched filaments (No. 1) → No. 4
	No. 6 undrawn filament	_____	→ No. 7	atonically annealed f.
	No. 8 undrawn filament → No. 9	heat stretching		
low density	undrawn filament	_____ → cold drawing (No. 10)	→ No. 10	{ atonically annealed f. isometrically annealed f.
Polyethylene medium density	undrawn filament	_____ → cold drawing (No. 11)	→ No. 11	{ atonically annealed f. isometrically annealed f.
high density	undrawn filament	_____ → No. 12	heat stretching	

a speed of 250 m/min, and treated by cold drawing as same as in sample No. 2, the resulted filaments heated as same as in the sample No. 5.

Sample No. 11; The sample was made from the medial density polyethylene, being as same as the sample No. 10 in the procedure.

Sample No. 12; Spinning method of this sample is as same as that of the sample No. 10, but the stretching treatment was done in a heated oven at 100°C, stretching speed being about 6 cm/min.

## B. Experimental Method

### 1. Density

The densities of polypropylene filaments were measured at  $20 \pm 0.1^\circ\text{C}$  with a density-gradient column prepared from methanol-water mixtures and calibrated with glass floats ranging in different densities from 0.860 to 0.950 g/cm<sup>3</sup>. Then the density was determined after 24 hours when its value became almost constant.

### 2. Refractive Index and Birefringence

Refractive indices  $n_{\parallel}$  and  $n_{\perp}$  of polypropylene filaments were measured at  $20 \pm 0.1^\circ\text{C}$  with Becke's line method using a polarized microscope. The letters  $n_{\parallel}$  and  $n_{\perp}$  show the refractive index for the monochromatic light (Na light) oscillating in the parallel direction to the fiber axis and in the perpendicular direction to the axis respectively, and  $n_{iso}$  which expresses the index of isotropic fiber was calculated by the following formula :

$$n_{iso} = \frac{1}{3} (n_{\parallel} + 2n_{\perp}) \quad (1)$$

Then, birefringence is :  $n_{\parallel} - n_{\perp}$

T. C. P-D. B. P (Tricresyl phosphate-Dibutyl phthalate) mixtures were used for immersion liquid, Each mixture was adjusted so as to have 0.001 interval of the refractive index. Becke's line was observed with the microscope just after immersion.

### 3. Birefringence in Heating Process

Changes of the retardation  $\Gamma$  and of the diameter  $D$  through the heating process were mesured on the microscope with a hot-stage; the former was determined by Quartz edge and the latter by the micrometer. Then, the birefringence is given the following formula.

$$\Gamma/D = n_{\parallel} - n_{\perp} \quad (2)$$

Rise and fall of temperature in the hot-stage was done with a rate of  $4^\circ\text{C}$  per minute, respectively.

### 4. X-ray Diffraction

X-ray diffraction patterns were developed with *Gigerflex* (D-6c) instrument equipped with a copper tube, a nickel oxide filter and Laue Camera. The

samples were bundles of about 36 parallel filaments, which were mounted in the instrument apart 3.9 cm from the camera. The X-ray beam was radiated perpendicular to the fiber axis.

The diffraction intensity along Debye-Scherrer ring at (110) plane was measured with Giger-counter. X-ray orientation of filaments was calculated from the half-width value in the diffraction intensity curve.

### III. RESULTS AND CONSIDERATIONS

#### 1. Relation between the density and the refractive index of polypropylene filament

The crystallinity of polypropylene filament was calculated by the following equation.<sup>16)</sup>

$$1/d = x/d_{cr} + (1-x)/d_{am} \quad (3)$$

Here,  $d$ : density of fiber,  $x$ : fraction of crystalline substance in fiber,  $d_{cr}$ : density of 100% crystalline polymer (0.936g/cm<sup>3</sup>),  $d_{am}$ : density of 100% amorphous polymer (0.858g/cm<sup>3</sup>)<sup>17)</sup>.

Then,

$$x = 12.82d - 10.999 \quad (3')$$

Gladstone-Dale's formula<sup>2)</sup> has been known to be very suitable to some kinds of polymers, which shows a qualitative relation between the density and the refractive index,

$$(n_{iso} - 1)/d = K \quad (4)$$

Here,  $n_{iso}$ : average refractive index,  $d$ : density,  $K$ : specific refractive energy.

Harmans<sup>3)</sup> has reported experimentally that the formula can be applied to the average refractive index of cellulose fibers. Therefore, if this formulary

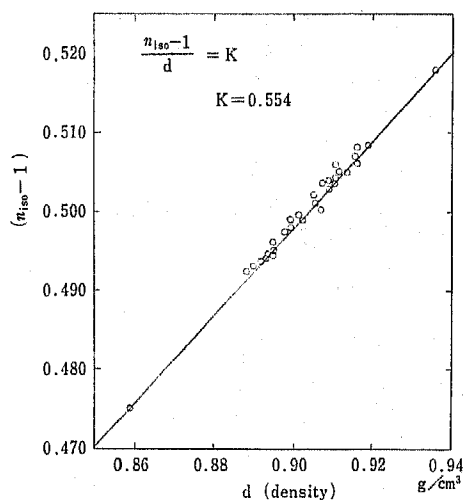


Fig. 1 Relation between density and refractive index

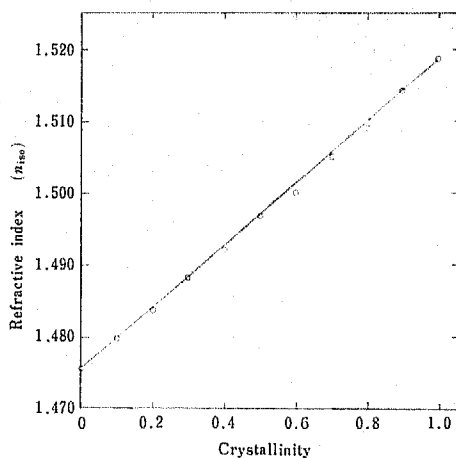


Fig. 2 Relation between refractive index and crystallinity

relation can be applied also to polypropylene filament, the crystallinity must be calculated by the refractive index of the filament.<sup>14)</sup>

From this point of view, the author measured the density and the refractive index of polypropylene filaments. The results obtained are denoted in Fig. 1.

In Fig. 1,  $(n_{iso}-1)$  is quite positively proportional to the density and  $K$  value is 0.554 by the experiment. Namely Gladston-Dale's formula is:

$$(n_{iso}-1)/d=0.554 \tag{4'}$$

From (3') and (4)', the following equation is given.

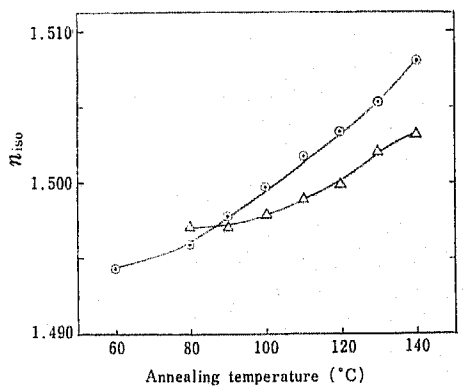
$$n_{iso}=0.043_2x+1.475_2 \tag{5}$$

Thus, the crystallinity can be calculated by the average refractive index. The relation between the crystallinity and the refractive index is shown in Fig. 2.

## 2. Optical properties of undrawn firaments

### a) The change of the optical property caused by heat treatment

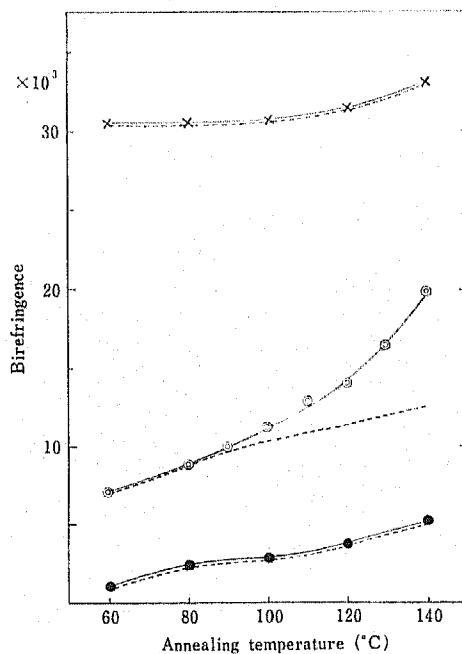
No. 1, samples of undrawn filaments (spinning draft : 250 times) were atonically annealed at 60, 80, 100, 120, 140 and 160°C for 30 min, and the sample of 4 times cold drawing were isometrically annealed at 80, 100, 120



—△— 4 times isometrically annealed filaments

—○— No. 4 and No. 7 samples.

Fig. 3 Change of  $n_{iso}$  caused by annealing



—×— : 4 times isometrically annealed filaments

—○— : No. 4 samples

—●— : No. 7 samples

Each broken line shows the change of birefringence only by crystallization.

Fig. 4 Change of birefringence caused by annealing

and 140°C for 30 min, in an oven, respectively. The results are shown in Fig. 3 and 4.

As shown in Fig. 3, the crystallinity indicated by  $n_{iso}$  increases remarkably according to heat treatments though it has no concern with the initial orientation of filaments. However, increasement of the crystallinity of 4 times isometrically annealed filaments was smaller than that of undrawn atonical ones.

Further, Fig. 4, shows that the birefringence increased with the raising temperature. And the increasing tendency of the birefringence is greatly effected by the initial orientation of the undrawn filaments.

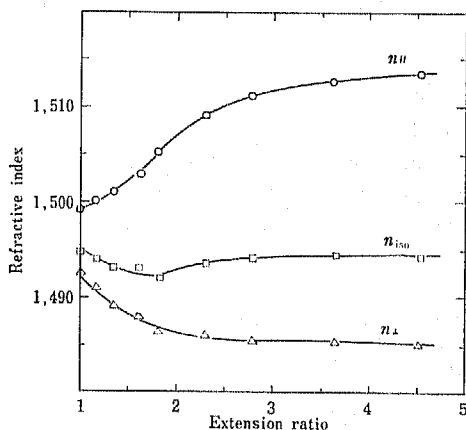


Fig. 5 Change of refractive indices caused by cold drawing

Meanwhile, the duration of heat treatment seems to have few effect on the crystallinity.

#### b) The change of optical property caused by cold drawing

The oriented filaments were prepared from No. 1 samples which were treated by cold drawing in various extension ratios at room temperature, and the changes of refractive indices of these filaments were measured by Becke's method. The results are shown in Fig. 5.

As extension ratio becomes larger,  $n_{//}$  and  $n_{\perp}$  become greater and smaller respectively, resulting the anisotropy increasement. The value of  $n_{iso}$ , however, decreased slightly at about 2-times extension ratio and here after it took almost the same value as the initial one. This phenomenon may be due to the break of the crystallite or to the formation of the void with extension.

By cold drawing, therefore, the increase of orientation is markedly while that of crystallinity is slightly.

#### c) The change of optical property caused by heat stretching

The change of refractive index and the birefringence of No. 3 samples which were obtained from the heat stretched<sup>10)</sup> samples of No. 1, is denoted in Fig. 6 and 7.

In heat stretching,  $n_{iso}$  increased at the temperature of 60°C to 100°C, on the contrary it tended to decrease at 120°C and above. But as a whole the crystallinity becomes larger with thermal raising in stretching. This fact seems due to a promotion of the crystallization by stretching, because the sheaf like crystal is easily formed following with parallel arrangement of the polymer chain from 60°C to 100°C, on the other hand, the folded crystal and sheaf like crystal are produced simultaneously at 120°C and above.

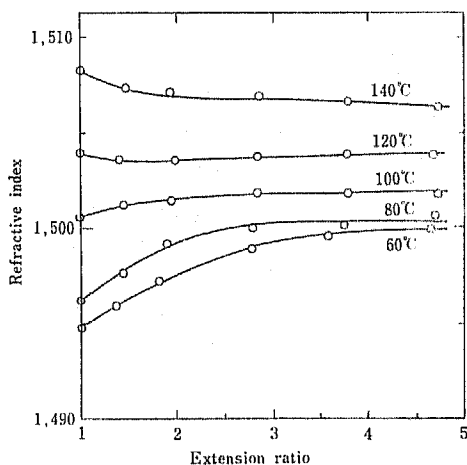


Fig. 6 Change of  $n_{iso}$  caused by heat stretching

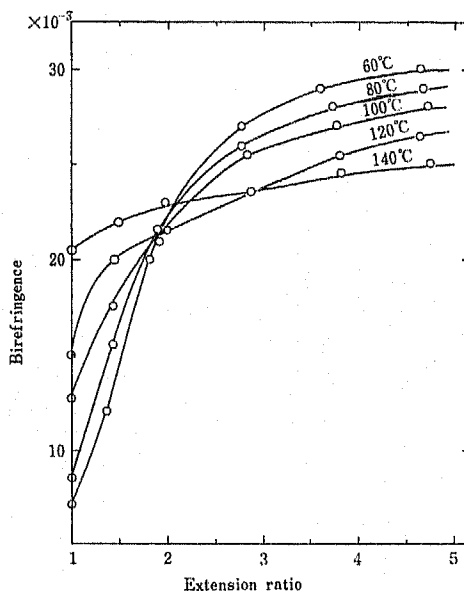


Fig. 7 Change of birefringence caused by heat stretching

The orientation effect by stretching is considerably larger at low temperature than at high temperature, because the noncrystalline parts are considered to have a larger fluidity at high temperature than low temperature.

#### d) The relation between $n_{//}$ and $n_{\perp}$

From the above-mentioned results, the relative diagram between  $n_{//}$  and  $n_{\perp}$  is summarized. It is shown in Fig. 8.

In Fig. 8 the line  $N$  ( $45^{\circ}$  to  $n_{\perp}$  axis) shows the change of  $n_{iso}$ . If the value of  $n_{iso}$  to crystal density  $d_{cr}$  ( $0.936 \text{ g/cm}^3$ ) and that to amorphous density  $d_{am}$  ( $0.858 \text{ g/cm}^3$ ) coincides respectively with 100% and 0% of crystallinity, the crystallinity of the polymer can be estimated by the value of  $n_{iso}$  on  $N$  line.

The line  $C$  ( $116^{\circ}$  to  $n_{\perp}$  axis) is given by  $n_{iso} = 1/3(n_{//} + 2n_{\perp})$ , so all data plotted on  $C$  line indicate to be equivalent in regard to the crystallinity.

The line  $O$  (about  $54^{\circ}$  to  $n_{\perp}$  axis) is, if plotted all data on  $O$  line, equivalent in regard to the orientation as well known in researches on cellulose<sup>12)</sup> and silk.<sup>4)</sup> Such a relationship in  $O$  line is presented in the later chapter on X-ray analysis.

In Fig. 8  $n_{//}$  and  $n_{\perp}$  of the cold drawn filaments (No. 2 sample) are plotted nearly on the line  $C$  and so little changes are recognizable in the crystallinity.

On the other hand,  $n_{//}$  and  $n_{\perp}$  of the unoriented filaments atonically annealed (No. 7 sample) and 4 times cold drawn filaments isometrically annealed come just on the line  $O$ . The above result shows that the orientation keeps a constant value though the crystallinity increases clearly.

When No. 1 samples are atonically annealed, the values of  $n_{//}$  and  $n_{\perp}$

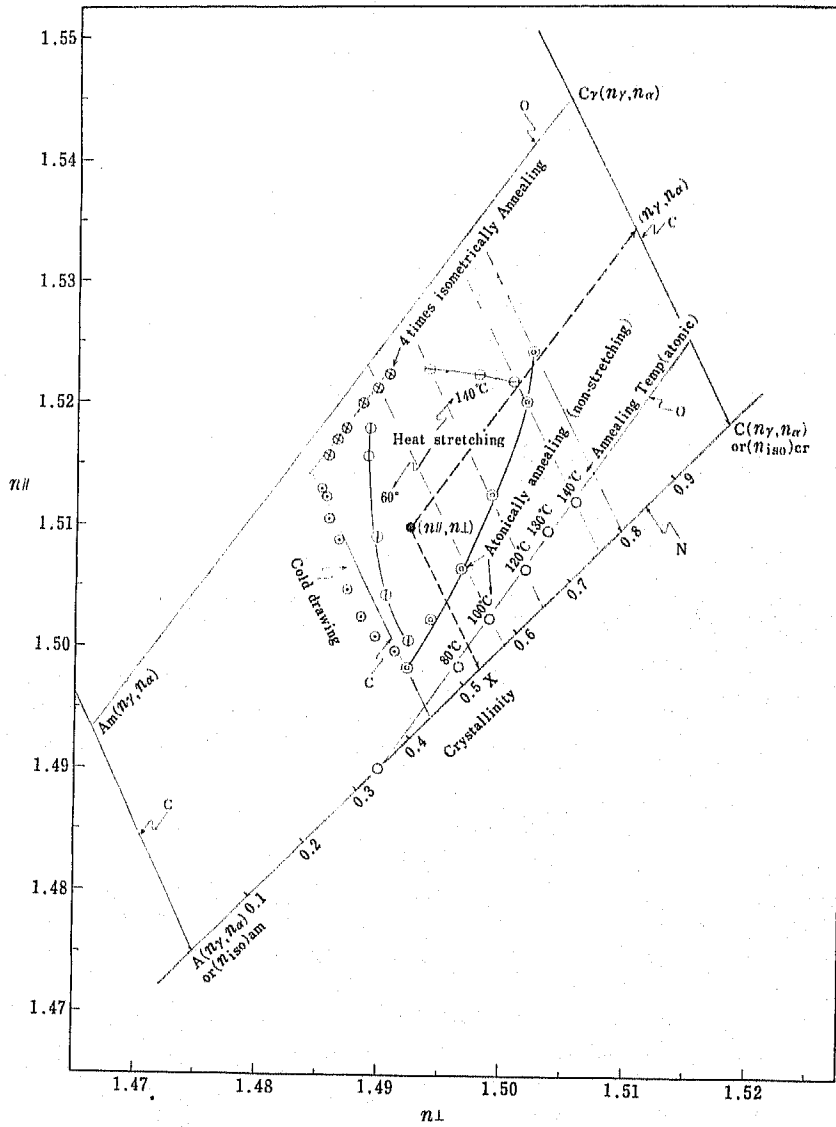


Fig. 8  $n_{//}$  and  $n_{\perp}$  diagram of polypropylene

do not agree with the line  $O$ , because the orientation increases remarkably with the crystallization.

With the increment of orientation, the crystallinity becomes larger in  $60^{\circ}\text{C}$  heat stretching while smaller in  $140^{\circ}\text{C}$  one.

Thus, Fig. 8 can reveal the relationship between crystallinity and orientation in various filaments. Further the above relationship will be given in Fig. 9 obtained from X-ray diffraction.



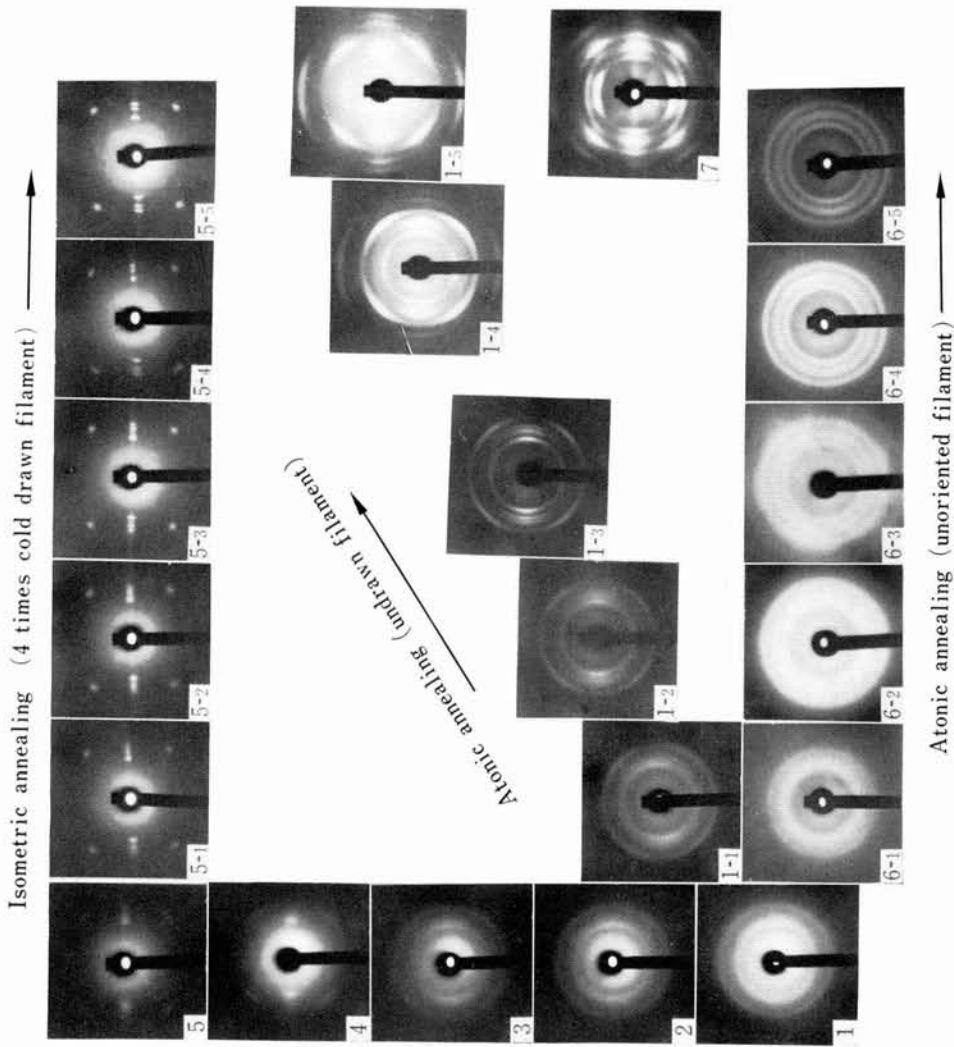


Fig. 9 X-Ray diffraction patterns by various treatments

Cold drawing (No.2 samples)

- 1 : 1 times (No.1 sample),
- 2 : 1.5 times, 3 : 2 times,
- 4 : 3 times 5 : 4 times,

Isometric Annealing (4 times cold drawn filament)

- 5-1 : 100°C 5-2 : 120°C
- 5-3 : 130°C 5-4 : 140°C
- 5-5 : 150°C

Atonic Annealing (No.4 samples)

- 1-1 : 60°C 1-2 : 80°C
- 1-3 : 100°C 1-4 : 140°C
- 1-5 : 160°C

Atonic Annealing (No.7 samples)

- 6-1 : 60°C 6-2 : 80°C
- 6-3 : 100°C 6-4 : 120°C
- 6-5 : 140°C

7 : Extruded filament in Glycerine (140°C)

Cold drawing ←

→ Atonic annealing (unoriented filament)

In Fig. 9, we can see the phase in which unoriented smectic diagram changes to oriented smectic diagram by cold drawing and in which undrawn and cold drawn samples (No. 1 and No. 2) change to monoclinic paracrystalline structure by above 100°C heat treatment.<sup>1)</sup>

By heat treatment, unoriented samples (No. 6 samples) and initial oriented samples (No. 1 sample) tend to increase the crystallinity and also the orientation and the crystallinity, respectively.

Four times isometrically annealed samples show a clear X-ray pattern according to crystallization though the orientation is constant, and the cold drawn or undrawn filaments which are annealed under a temperature close to the melting point have *a* axis orientation, on the contrary the previous paracrystalline samples had *c* axis orientation.

### 3. The change of birefringence in polypropylene filaments through heating process

The optical properties of undrawn filaments afore-mentioned were concerned to those which were resulted from various treatments.

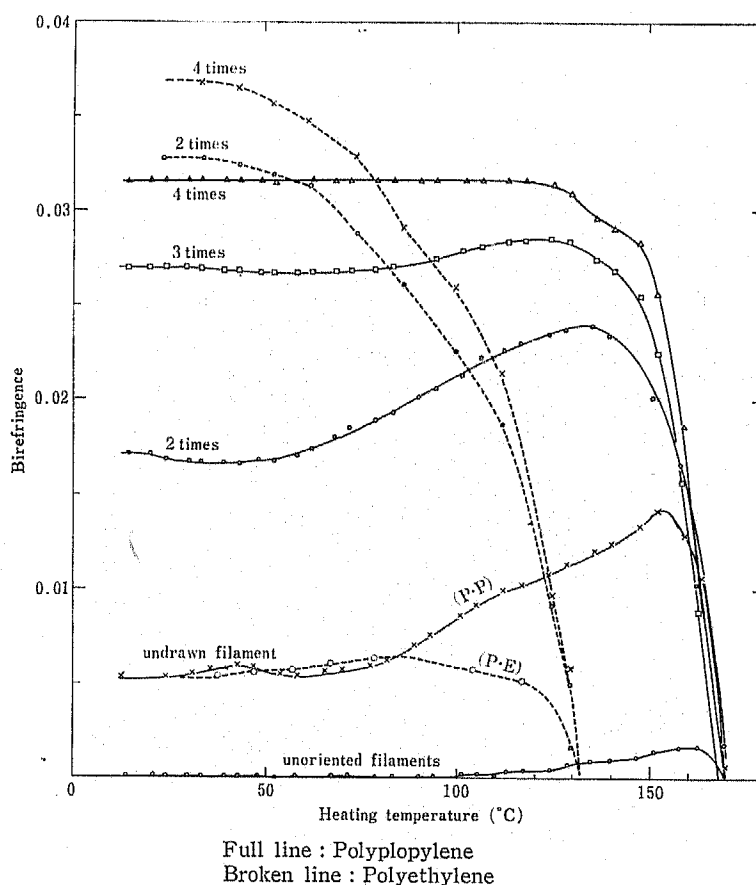


Fig. 10 Change of birefringence in cold drawn polyolefine filaments through heating process

In this time the author tried to examine the optical behavior along a process of heat treatment. Such an experiment must contribute to a key for analysis of fine structure of fibers.

**a) The optical behavior along a heating process in various cold drawn filaments**

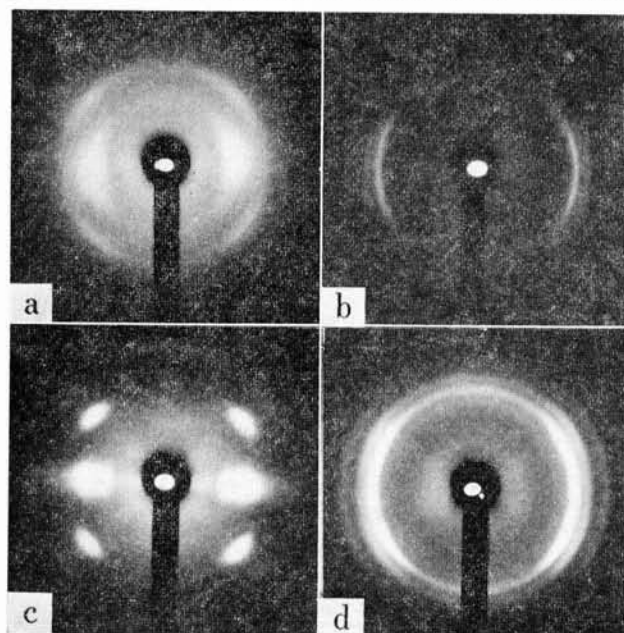
The change of birefringence in heating process was measured on the drawn and unoriented polypropylene filaments and on the drawn polyethylene filaments. The results are shown in Fig. 10.

In the undrawn filaments, the birefringence of unoriented sample (No. 6) increased slightly with heating, but that of the slightly initially oriented sample (No. 1) began to increase strikingly near at 80°C showing the maximum value at nearly below the melting temperature and after disappeared rapidly.

The cold drawn samples take nearly the same behavior as in No. 1 samples. The rate of increase in birefringence decreases adverse to increase-ment of extension ratio, though a heavy extension ratio does not bring such a phenomenon.

Each peak of birefringence curves tends to move toward lower temperature with increasement of extension ratio.

On the other hand, in the undrawn polyethylene filaments which have



a (P.P) b (P.E) : Before atonic annealing  
 c (P.P) d (P.E) After atonic annealing  
 (at 100°C for 30 min)

**Fig. 11** X-ray diffraction patterns caused by atonic annealing of 2 times cold drawn filaments

the initial orientation the above phenomenon does not occur so evidently as in polypropylene. In the low extension samples the birefringence decreases greatly along heating process.

The optical behavior of polyethylene and polypropylene along heating process are adversely different from each other.

Fig. 11 shows X-ray patterns of both polymers which were treated by 2 times cold drawing and taken up after heating.<sup>7)8)</sup>

In Fig. 11, when these samples annealed at 100°C for 30 min, polypropylene changes to the crystallized and oriented X-ray diagrams (monoclinic) from the low crystallized and low oriented ones (smectic), without change of *c* axis orientation. Polyethylene, however, changes to the oriented X-ray diagram with *a* axis orientation.

From these fact, it is recognized that annealed cold drawn samples of polypropylene tend to have *c* axis orientation, while those of polyethylene have *a* axis orientation.

#### b.) The optical behavior through heating and cooling process

The cooling treatment was given to 2 times cold drawn samples on the way of heating process until the cooling temperature reached 20°C and after the samples were reheated. In this way, the birefringence was measured.

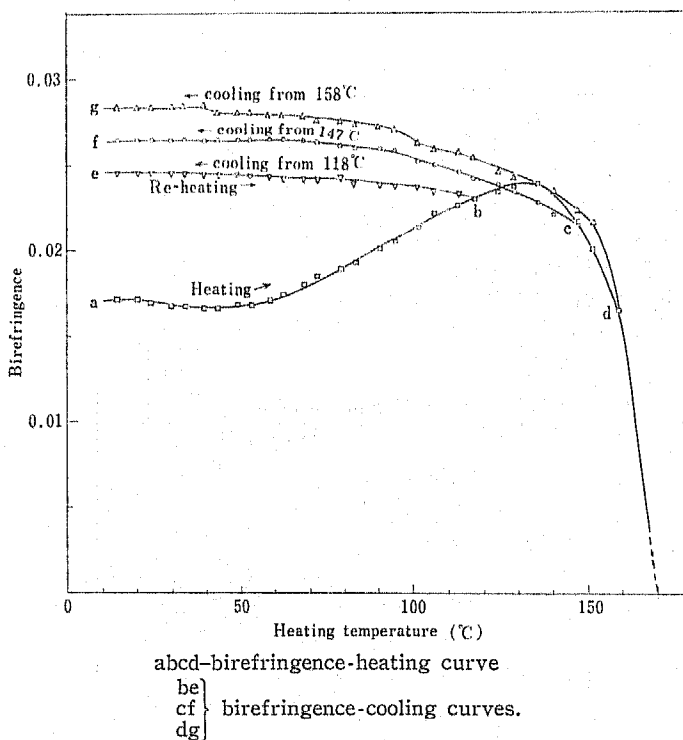


Fig. 12 Change of birefringence through heating and cooling process of 2 times cold drawn filaments

The results obtained are shown in Fig. 12.

When the above treatment was done, the birefringence does not resume its curve and takes a different direction increasing its value. Further, when the same treatment was done at higher temperature in heating process the birefringence becomes larger at room temperature.

If these samples cooled at room temperature are reheated, the birefringence traces the previous curve in the cooling process resuming to its cooling position and it traces again the original heating curve.

Such a behavior of the birefringence appears unchangeably even though this heating-cooling operation is carried out repeatedly.

Even if the sample is cooled near at the melting point over the maximum birefringence in heating, the birefringence keeps a large value at room temperature.

### c) The change of length in heating process

The change of length of cold drawn samples was microscopically measured under heating procedure. The results are shown in Fig. 13.

The undrawn filaments (No. 1 sample) elongate themselves in length and shrink markedly near at the melting point. The low extension samples shrink firstly, next elongate naturally and again shrink remarkably at about

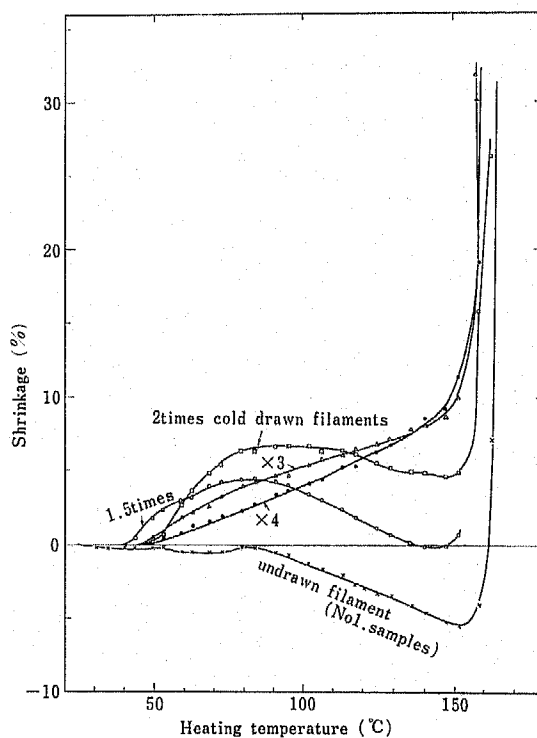


Fig. 13 Change of length in heating procedure of cold drawn polypropylene filaments

melting temperature, but the high extension samples shrink gradually.

Considered from this phenomenon and optical behavior indicated in Fig. 11 and 12, the undrawn samples used in this experiment have a faint initial orientation, so that  $c$  axis of the crystal orients slightly toward the direction of the fiber axis, and the crystallites grow up to the direction of the fiber axis with annealing.

The development of the crystalline region, therefore, will make the oriented component increase in the direction of the fiber axis. This assumption will contribute to the phenomenon that the birefringence increase conspicuously together with the natural elongation.

In the low extension samples the folding crystalline parts are unfolded by stretching, and at the same time the crystalline and the unfolded parts orient toward the direction of the fiber axis. The unfolded parts of these samples are folded up in the original crystal by heat treatment.

In the high extension samples, the polymer chain axis unfolded freely from folding crystalline parts orients parallel to the stretching direction, changing to the sheaf like crystal ( $c$  axis orients toward the stretching direction).

The sheaf of crystal melts partially under heating process, and then the folded crystal is formed. This will be the causation of shrinkage of filaments.

A striking shrinkage which happens at about the melting temperature seems to be caused by the melt of the crystallite ( $a$  axis orientation appears partially).

Thus, the shrinkage, the natural elongation and the increase of birefringence by heat treatment can be explained from a qualitative relationship between orientation and crystallization.

Now, we must pay our attention on the heating-cooling curves in Fig. 12. In it, these curves show that there is likely little difference between the orientation of melted part and that of unmelted part, and so the birefringence increases at room temperature, nevertheless, in fact the orientation of melted part takes a descent curve, on which the author will mention in the later chapter.

#### 4. Analysis of fiber structure by $n_{//}$ and $n_{\perp}$ diagram

##### a) Experiment on the equivalent orientation line

The explanation of  $n_{//}$  and  $n_{\perp}$  diagram has already been given in Chapter 2-d, in which every plot on line  $O$  of Fig. 8 has been known experimentally to be equivalent in regard to the orientation.

Then, each mean value of orientation factors obtained by X-ray diffraction was compared with each corresponding value on line  $O$ , respectively. Table 2, shows the relation between this orientation factor and the birefringence obtained by Becke's method.

Table 2. Relation between birefringence and X-ray orientation

Annealing temperature (°C)	60	80	100	120
$n_{//}$	1.518	1.521	1.523	1.526
$n_{\perp}$	1.487	1.489	1.491	1.493
$n_{iso}$	1.497 <sub>3</sub>	1.499 <sub>7</sub>	1.501 <sub>7</sub>	1.504
$n_{//} - n_{\perp}$	0.031	0.032	0.032	0.033
$\pi$	0.92 <sub>5</sub>	0.92 <sub>7</sub>	0.92 <sub>7</sub>	0.92 <sub>7</sub>

The mean value of orientation factor is nearly stable though the birefringence increases.

b) The change of birefringence in crystalline and non-crystalline regions considered from  $n_{//}$  and  $n_{\perp}$  diagram

Generally, the birefringence of fiber is given by the following formula.

$$\Delta n = \Delta n_{cr}x + \Delta n_{am}(1-x) \quad (6)$$

Where,  $\Delta n$ : birefringence of fiber,  $x$ : fraction of crystalline material in fiber,  $\Delta n_{cr}$ : birefringence of crystalline region,  $\Delta n_{am}$ : birefringence of non-crystalline region.

In Fig. 8 the line C of 100% crystallinity contains the refractive indices of the unorientated crystallite and those of the crystalline of perfectly parallel orientation. The birefringence can be calculated by the difference between  $n_{//}$  and  $n_{\perp}$  which are obtainable from the diagram. Therefore, we can reduce the refractive index on the line C into each birefringence value from perfectly unoriented crystalline region to perfectly oriented one.

An intersection point between a straight line O (54° to  $n_{\perp}$  axis) through

an optional point ( $n_{//}$ ,  $n_{\perp}$ ) and the line C of 100% crystal gives each refractive index ( $n_r$ ,  $n_a$ ) of crystalline region in an optional samples, the difference between both the indices showing the birefringence of crystalline region, which is shown as  $\Delta n_{cr}$  in (6) equation.

An intersection point between a straight line C (116° to  $n_{\perp}$  axis) through an optional point ( $n_{//}$ ,  $n_{\perp}$ ) and line N (45° to  $n_{\perp}$  axis) shows the crystallinity ( $x$ ) calculated from the value  $n_{iso}$ . Then the birefringence of noncrystalline region can be calculated by (6) equation.<sup>13)</sup>

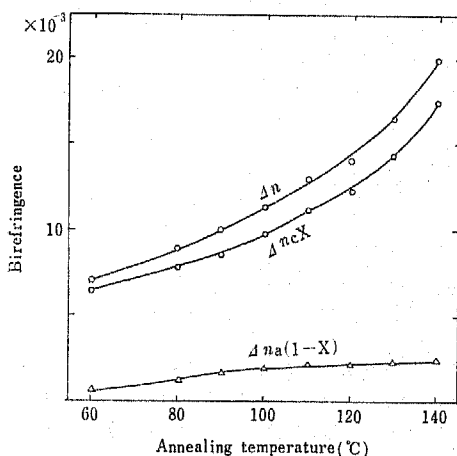


Fig. 14 Change of birefringence in crystalline and non-crystalline region caused by atonic annealing on the undrawn filaments

c) The change of birefringence in crystalline and non-crystalline regions caused by annealing, cold drawing and heat stretching

In this section the author desires to estimate the change of birefringence in the crystalline and noncrystalline region from  $n_{\parallel}$  and  $n_{\perp}$  diagram referring the results mentioned in Chapter 2-a. b. c.

Fig. 14 in which the atonic annealing as treated undrawn filaments indicates that the birefringence of the crystalline region increases more significantly than that of non-crystalline region.

In the cold drawing (Fig. 15), a large increment of the birefringence in the crystalline region appears at the low extension ratio, while that in non-crystalline region occurs at high extension ratio.

In heat stretching (Fig. 16), the value of the initial birefringence in high temperature stretching is larger than that in the low temperature one, though each difference between birefringence in crystalline region tends to be smaller as the extension ratio increases. On the other hand, an increase of birefringence in the non-crystalline region is a little at high temperature stretching.

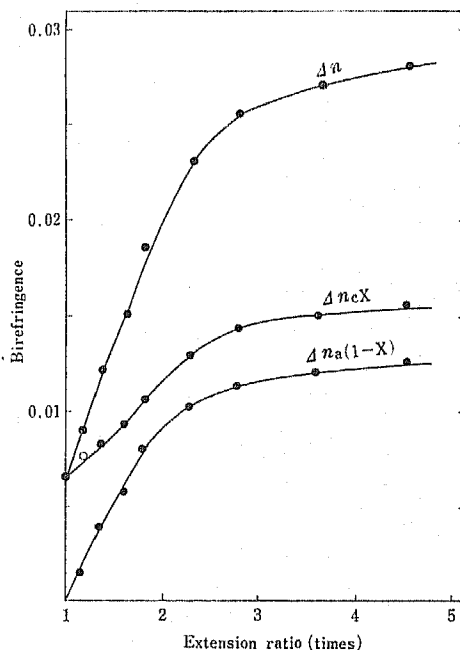


Fig. 15 Change of birefringence in crystalline and non-crystalline region caused by cold drawing

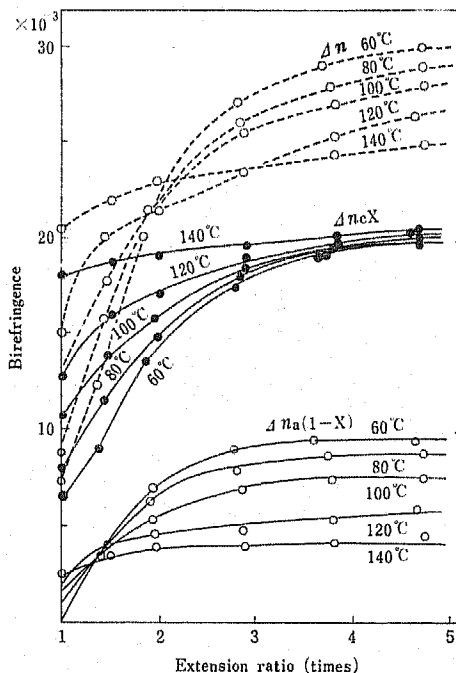


Fig. 16 Change of birefringence in crystalline and non-crystalline region caused by heat stretching



d) The change of optical properties caused by isometric and atonic annealing to cold drawing filaments

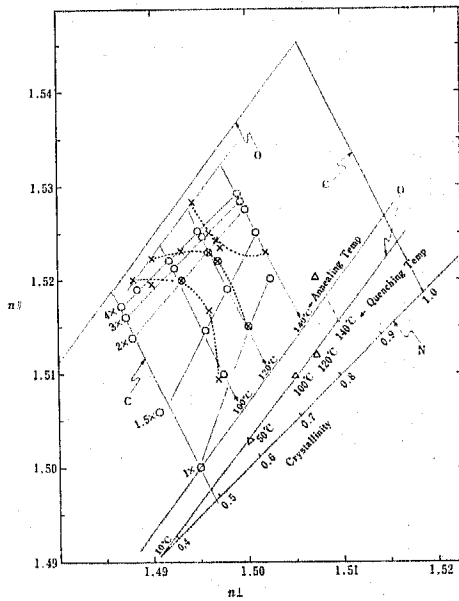
Polypropylene

The cold drawn filaments (No.2. sample) were annealed under the isometric and the atonic conditions<sup>9)15)19)</sup> at various temperature and their refractive indices were measured. The relation between  $n_{\parallel}$  and  $n_{\perp}$  is shown in Fig. 17.

The crystallinity of the samples annealed atonically (No. 4 sample) is determined by the thermal factor. With increment of treating temperature, the orientation of the samples which were stretched 2 times and more tends to decrease, while that of the lower extended samples increases.

In high stretched treatments, the crystallinity in the isometrically annealed samples is less than that in the atonically annealed ones. The effect brought by the fixation of orientation was found in the four times isometric samples, but in the other isometric samples such an effect was not recognized showing the same tendency as in atonic samples.

Furthermore the results in the case of four times atonically annealing



—●— cold drawn filaments  
 —○— atonically annealed filaments  
 —×— isometrically annealed filaments  
 —△— quenched undrawn filaments in glycerine

Fig. 17 Change of  $n_{\parallel}$  and  $n_{\perp}$  caused by isometric and atonic annealing of cold drawn polypropylene filaments

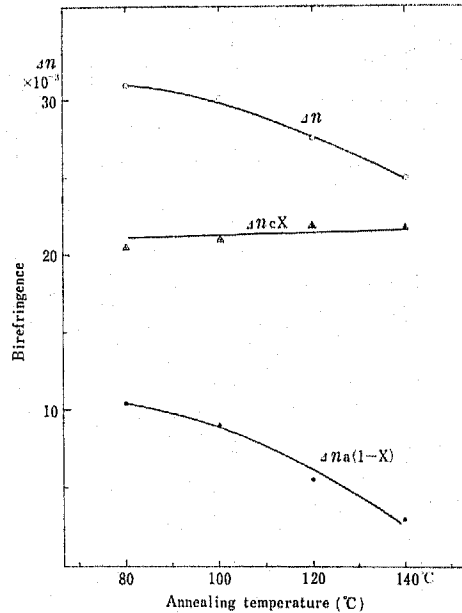


Fig. 18 Change of birefringence of crystalline and non-crystalline region caused by atonic annealing of 4 times cold drawn filaments

are shown in Fig. 18.

The birefringence of the filaments decreases as the temperature becomes higher. It seems to be caused by a decrease of birefringence in the non-crystalline region, besides the change of birefringence in the crystalline region is little.

### Polyethylene

The author has found that the Gladstone-Dale's equation is applicable to polyethylene as same as polypropylene. The value of  $K$  was 0.554. In this time the cold drawn filaments were annealed under the isometric and the atonic conditions, and measured the change of the refractive indices.<sup>17)18)</sup> The obtained results are shown in Fig. 19.

The crystallinities of isometrically and atonically annealed samples increase. The orientation of atonically annealed samples decreases obviously while that of isometric samples increases. The refractive indices of these samples do not appear on the line  $C$  ( $54^\circ$  to  $n_{\perp}$  axis) except in isometric samples of the high orientation.

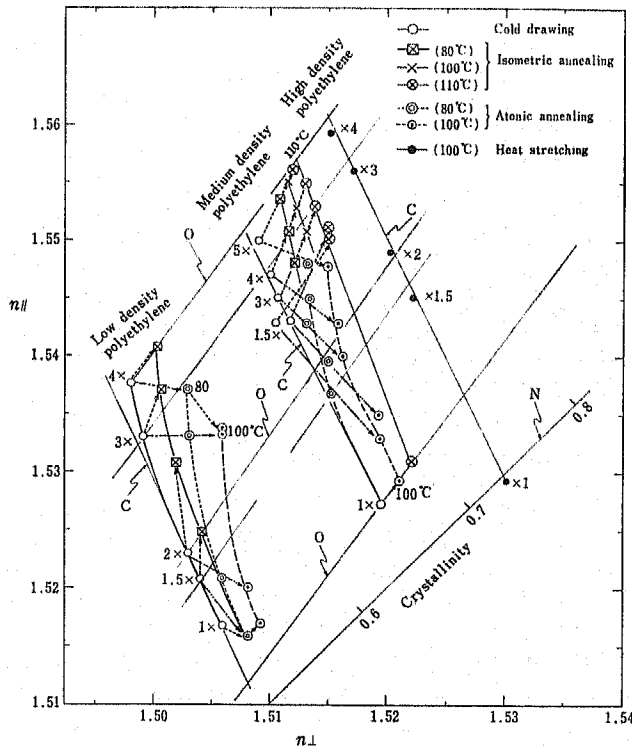
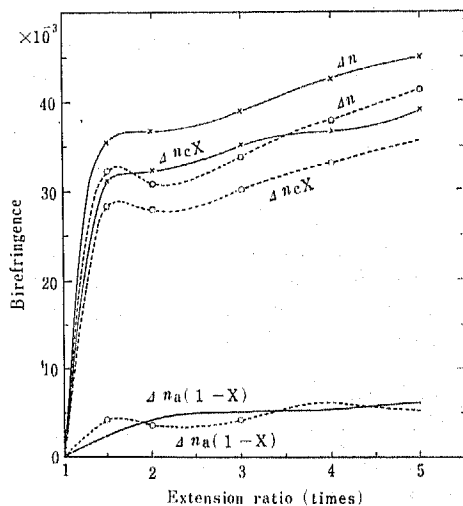
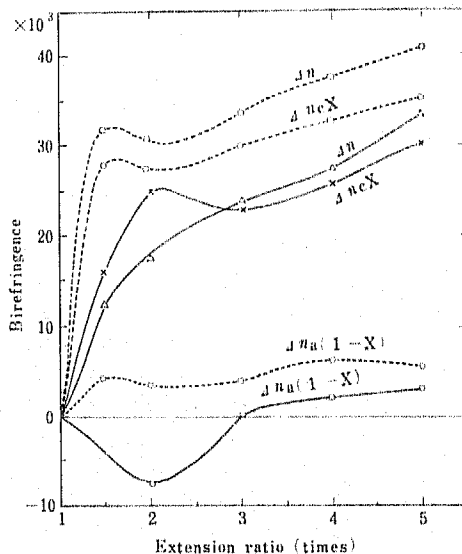


Fig. 19 Change of  $n_{//}$  and  $n_{\perp}$  caused by isometric and atonic annealing of cold drawn polyethylene filaments



Broken line; before treatment  
Full-line; after treatment

Fig. 20 Change of birefringence in crystalline and non-crystalline region caused by isometric annealing of cold drawn filaments



Broken line; before treatment  
Full-line; after treatment

Fig. 21 Change of birefringence in crystalline and non-crystalline region caused by atonic annealing of cold drawn filaments

Probably, the above fact means that the structural molecular orientation of the cold drawn filaments is not uniform partially and the chain molecule itself tends to take  $a$  axis orientation at high temperature, though these filaments seem likely to take a uniform orientation from external observation.

The change of birefringence these filaments in crystalline and non-crystalline regions is illustrated in Fig. 20 and 21.

Fig. 20 shows that the birefringence of crystalline region increases with isometric annealing, and Fig. 21 shows that non-crystalline region has  $a$  axis orientation with atonic annealing.

In both figures each birefringence-extension curve has an abnormal part when cold drawing ratio is about 1.5 times. It suggests that folded crystalline parts in filaments may be unbound and many unstable molecules which are unfixed in the crystalline region may be produced in non-crystalline region, because a slight decrease of  $n_{iso}$  by cold drawing, a disappearance of the abnormal part by isometric annealing and  $a$  axis orientation of non-crystalline region by atonic annealing occur at the extension ratio of about 1.5 times.

#### e) The change of refractive index caused by spinning condition of polypropylene

The extruded monofilaments (No. 8 sample) were quenched in a glycerine bath respectively at 50, 100, 120, and 140°C and taken up with a speed of

250 m/min. These undrawn filaments have a slight birefringence. The refractive indices of these samples were plotted in Fig. 17 and X-ray photograph of the filaments quenched at 140°C was shown in Fig. 9-7.<sup>5)6)</sup>

The quenched undrawn filaments have larger crystallinity and  $a$  axis orientation than atonically annealed filaments in the same thermal condition.

Now, we must take out notice to the following fact in Fig. 9. It is that  $n_{//}$  and  $n_{\perp}$  diagram is possible to be divided into three parts such as smectic content,  $c$  axis orientation and  $a$  axis orientation according to conditions such as spinning, heating and stretching. Therefore, an occurrence of crystal transformation can be easily detected by this diagram.

#### IV. CONCLUSION

Fine structures of undrawn and drawn isotactic polypropylene filaments were investigated using density, refractive index, birefringence and X-ray diffraction, and the author reached to the following conclusions.

1) The relation between density and refractive index in polyolefine filaments is expressed suitably by Gladstone-Dale's equation  $(n_{iso}-1)/d = 0.554$  and the crystallinity of polymer can be calculated by the refractive index ( $n_{iso}$ ).

2) The interrelation between the crystallinity and the orientation of polymer under heat treatment, cold drawing and heat stretching can be estimated from  $n_{//}$  and  $n_{\perp}$  diagram. It was proved by comparison of  $n_{//}$  and  $n_{\perp}$  diagram with X-ray diffraction.

3) The crystallinity of undrawn filaments is determined by the thermal factor in quenching or annealing treatment. The crystalline region in undrawn filaments has a folding structure. The determinant of the initial orientation in undrawn filament is spinning draft. In this case, the orientation component is seen mainly crystalline region and not in non-crystalline region, of which the orientation is at random. The higher quenching or annealing temperature is, the more  $a$  axis orientation increases in the orientation component.

4) The crystallinity in drawn filaments is determined by the thermal factor as same as in undrawn filaments, but the structure of crystalline region, according to stretching rate, changes from a low orientation with folded crystal which is mixed with sheaf like crystal, to a high orientation with sheaf like structure. This sheaf like crystal is unstable in heat being apt to change to folding crystal when melted.

5) Heat stretching under lower than the optimum crystallization temperature promotes the sheaf like crystallization, while that under higher than the optimum temperature reduces this crystallization because folding crystal (arranging toward  $c$  axis) and sheaf like crystal (arranging toward  $c$  axis) are produced simultaneously.

6) The orientation of drawn filaments is mainly in  $c$  axis, but  $a$  axis orientation appears partially in high heat stretching. From this fact, the reason why the line  $O$  (54° to  $n_{\perp}$  axis) which is applicable to regenerated

cellulose or silk fibroin filaments could not be applied to the other samples except to the isometric samples with high orientation, seems to be caused by a difference of folding structure between each samples.

7) The phenomenon of natural elongation and shrinkage by heat treatment is presumed to be brought by folding crystallization considering from changes of birefringence through heating process.

8) The author presented here the analyzing method of birefringences of crystalline and non-crystalline regions from  $n_{\parallel}$  and  $n_{\perp}$  diagram. The further study on this diagram will be contributed to the analysis of fiber structure.

### Acknowledgments

The author wishes to thank Professor Dr. Y. Go for much valuable advice during the work, and Professor Dr. N. Koyama for many different kinds of aid in the preparation of the manuscript.

Thanks are also due to Messrs Y. Kato, H. Kanai, M. Tsuji and Miss. H. Hashizume who assisted this study. The materials used for this work were given from Mitsubishi Rayon Company, for which the author acknowledges deeply.

### Literatures cited

- 1) Farrow. G : J. Appl. Polymer Sci. 9, 1227 (1965)
- 2) Gladston and Dale : Phil. Trans 153, 317 (1863)
- 3) Hermans. P. H : Contribution to the physics of cellulose Fibers Elsevier (1946)
- 4) Ishikawa. H and Kubota. J : Res. Reports. Faculty. Text. Shinshu Univ. 5, 97 (1955)
- 5) Ishizuka. O : J. Soc Text and cell Ind. Japan 18, 198 (1962)
- 6) Ishizuka. O, Matsumura. O, Kobayashi. K and Horio. M : J. Soc. Chem. Ind. Japan 65, 143 (1962)
- 7) Kinoshita. S and Takizawa. T : Chem, High Polymers 17, 32 (1960)
- 8) Kinoshita. S and Takizawa. T : Chem, High Polymers 19, 397 (1962)
- 9) Kuribayashi. S and Nakai. A : J. Soc. Text and cell. Ind. Japan 18, 64 (1962)
- 10) Nakai. A., Yoshikawa. S and Oya. S : J. Soc. Text and cell. Ind. Japan 17, 997 (1961)
- 11) Natta. G., : J. Polymer Sci 16, 143 (1955)
- 12) Okajima. S and Kobayashi. Y : J. Soc. Chem. Ind. Japan 46, 941 (1943)
- 13) Samuels. R. J. : J. Polymer Sci, A3, 1741 (1965)
- 14) Schael. G. W. : J. App. Polymer Sci 8, 2717 (1964)
- 15) Sheehan. W. G., Wellman. R. E. and Cole. T. B : Text. Res. J. 7, 626 (1965)
- 16) Sobue. H and Tabata. Y., : J. App. Polymer Sci 2, 62 (1959)  
Sobue. H and Tabata. Y., : J. App. Polymer Sci 2, 66 (1959)  
Sobue. H and Tabata. Y. : J. Polymer Sci 39, 427 (1959)
- 17) Stein. R. S and Norris F. H : J. Polymer Sci 21, 381 (1956)
- 18) Stein. R. S : J. Polymer Sci. 31, 327 (1958)
- 19) Wyckoff. H. W. : J. Polymer Sci 62, 83 (1962)